# Flexible electrically pumped random lasing from ZnO nanowires based on metal–insulator–semiconductor structure*

Miao-Ling Que(阙妙玲), Xian-Di Wang(王贤迪), Yi-Yao Peng(彭轶瑶), and Cao-Feng Pan(潘曹峰)†

*Beijing Institute of Nanoenergy and Nanosystems, Chinese Academy of Sciences, National Center for Nanoscience and Technology (NCNST), Beijing* 100083, *China*

(Received 7 April 2017; revised manuscript received 10 April 2017; published online 10 May 2017)

Flexible electrically pumped random laser (RL) based on ZnO nanowires is demonstrated for the first time to our knowledge. The ZnO nanowires each with a length of 5 μm and an average diameter of 180 nm are synthesized on flexible substrate (ITO/PET) by a simple hydrothermal method. No obvious visible defect-related-emission band is observed in the photoluminescence (PL) spectrum, indicating that the ZnO nanowires grown on the flexible ITO/PET substrate have few defects. In order to achieve electrically pumped random lasing with a lower threshold, the metal–insulator–semiconductor (MIS) structure of Au/$SiO_2$/ZnO on ITO/PET substrate is fabricated by low temperature process. With sufficient forward bias, the as-fabricated flexible device exhibits random lasing, and a low threshold current of ∼ 11.5 mA and high luminous intensity are obtained from the ZnO-based random laser. It is believed that this work offers a case study for developing the flexible electrically pumped random lasing from ZnO nanowires.

**Keywords:** flexible, random laser, ZnO nanowires, MIS structure

**PACS:** 73.20.Mf, 78.67.Uh, 73.40.Qv **DOI:** 10.1088/1674-1056/26/6/067301

## 1. Introduction

ZnO has received widespread attention as a promising material for photoelectric devices due to its direct wide band gap ($E_g = 3.37$ eV) and a relatively large exciton binding energy (60 meV).[1,2] Diverse researches based on ZnO have been reported such as light-emitting diodes (LED),[3–5] random lasers,[6–8] waveguide lasers,[9,10] etc. Among them, random lasing is an interesting optical phenomenon caused by multiple scattering in disordered gain medium, with great potential applications in display and imaging. Since the optically pumped RL based on ZnO powders[11,12] and ZnO polycrystalline films[13,14] was reported by some groups, RL from ZnO has attracted extensive research interest recently. In order to implement practical application of RL, electrically pumped RL from ZnO film or ZnO nanowires/nanorods has been widely studied.[15–17] Comparing with the ZnO film, there are some interspaces among the ZnO nanowires/nanorods. This makes it possible to modify the spatial variation of refractive index ($n_r$) for the ZnO nanowires/nanorods by filling other materials with different values of $n_r$. Therefore, ZnO nanowire/nanorod arrays are superior to ZnO film in the performance of optical scattering.[18] In addition, the grain boundaries in ZnO film will hinder the transportation of carriers in ZnO, which will reduce the luminous efficiency of the device greatly. In contrast, the ZnO nanowires/nanorods tend to possess less grain boundaries than the ZnO film, which will provide a smoother pathway for the carriers transportation, and this is favorable for enhancing the luminescence and suppressing the optical loss.

On the other hand, up to now, nearly all of the RL from ZnO were fabricated on the stiff substrates, such as GaN, $Al_2O_3$, glass and Si,[19–22] the lack of flexibility with a stiff substrate prevents the RL devices from going into service such as smart skin, foldable electronics,[23] lightweight products, etc.[24,25] Therefore, a flexible electrically pumped RL becomes indispensable and will present a huge potential application in the future electronics.[26,27]

In this paper, flexible electrically pumped random lasing from ZnO nanowires is demonstrated for the first time. We synthesize the ZnO nanowire arrays by hydrothermal process, then deposit $SiO_2$ film and Au film successively to construct the MIS structure. Forward bias is applied to the as-fabricated device, and with the increase of applied voltage, the device exhibits near band emission (NBE) under low injection current and then random lasing under higher injection current. A low threshold injection current of ∼ 11.5 mA and a stable output power are obtained from the random lasers based on ZnO nanowires.

*Project supported by the National Natural Science Foundation of China (Grant Nos. 61405040, 61675027, 51622205, 51432005, 61505010, and 51502018), the National Key Research and Development Project, Ministry of Science and Technology, China (Grant No 2016YFA0202703), the National Postdoctoral Program for Innovative Talents, China (Grant No. BX201600040), the China Postdoctoral Science Foundation (Grant No. 2016M600976), and the "Thousand Talents" Program of China for Pioneering Researchers and Innovative Teams.

†Corresponding author. E-mail: cfpan@binn.cas.cn

© 2017 Chinese Physical Society and IOP Publishing Ltd 

## 2. Experimental section

### 2.1. Fabrication of the device

Figure 1 depicts the detailed fabrication procedure of the flexible MIS device based on the ZnO nanowire arrays synthesized on the ITO/PET substrate (a resistivity of $\sim 28\ \Omega$·cm). Firstly, acetone, isopropyl alcohol, and deionized water were used successively to ultrasonically clean the ITO/PET substrate, and then nitrogen gas was used to blow dry the substrate (Fig. 1(a)). Secondly, we deposited a 70-nm thick ZnO film as the seed layer on the ITO/PET substrate by AC reactive magnetron sputtering as shown in Fig. 1(b). Subsequently, the substrate with ZnO seeds was placed into aqueous solution containing 40-mM/L zinc nitrate hexahydrate and 40-mM/L hexamethylenetetramine, after the chemical reaction at 85 °C in the oven for 4 h, the ZnO nanowire arrays were grown upward on the flexible ITO/PET substrate as shown in Fig. 1(c).[28] Immediately following the synthesis of ZnO nanowires, we spun SU-8 photoresist to fill the interspaces among the ZnO nanowires, and etched away the top of the SU-8 by oxygen plasma with the purpose of exposing the heads of ZnO nanowires (Fig. 1(d)). Subsequently, a 150-nm thick $SiO_2$ film was deposited on the top of ZnO nanowires by electron beam evaporation as revealed in Fig. 1(e). Finally, figure 1(f) shows that an 80-nm thick and a 120-nm thick Au films were sputtered onto the $SiO_2$ film and the exposed ITO/PET substrate as the top and bottom electrodes, respectively.

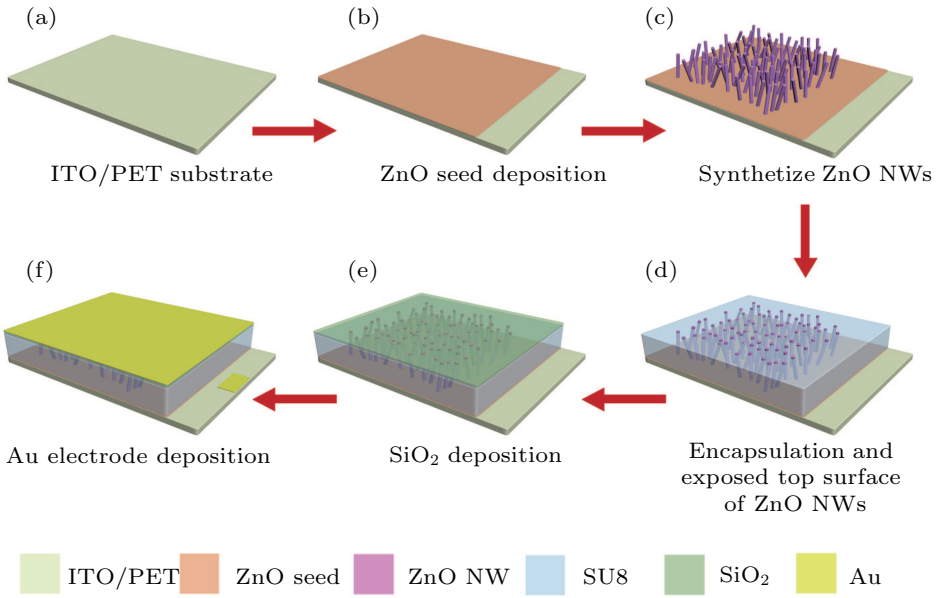



**Fig. 1.** (color online) Schematic diagram of the fabrication procedure of a flexible random laser based on ZnO NWs/$SiO_2$/Au.

### 2.2. Characterization

The morphology and crystal quality of the synthesized ZnO nanowires were characterized by field-emission scanning electron microscope (FESEM, Hitachi SU8020) and high-resolution transmission electron microscopy (HRTEM) (FEI Tecnai G20). X-ray diffraction (XRD) patterns were collected by an x-ray diffractometer (PANalytical X'Pert 3 Powder) with a Cu K$\alpha$ radiation source. The room-temperature photoluminescence (PL) spectra of the devices were acquired excited by a nanosecond pulsed laser (355 nm). Upon a forward bias, the electroluminescence (EL) characteristics of the flexible devices were obtained, with the positive voltage applied to the top electrode, while the negative voltage applied to the bottom electrode (ITO/PET). The current-voltage curve was obtained using the Keithley 4200 SCS system. The flexible random lasers were powered by Maynuo DC Source Meter M8812 and the EL spectra of the devices were captured by spectrometer Horiba iHR550. The Zeiss Observer microscope equipped with an HQ2 camera was used to take the lighted-up images of the flexible random lasers.

## 3. Results and discussion

### 3.1. Device structure and materials characterization

Figure 2(a) shows the structure diagram of a flexible MIS device based on the ZnO nanowire arrays on ITO/PET substrate. With a thickness of the whole device of about 500 μm, the flexible random laser exhibits high bendability as shown in Fig. 2(c). Figures 2(d) and 2(e) exhibit the top-view and cross-sectional FESEM images of the as-fabricated ZnO nanowires on ITO/PET substrate, which indicate that the ZnO nanowires are 5 μm in length and about 180 nm in average diameter. The microstructure and crystallinity of the hydrothermally synthesized ZnO nanowires are investigated by TEM and XRD. Figure 2(b) shows the XRD pattern of the as-grown ZnO nanowires and the only remarkable peak centered

at 34.49° can be well indexed to (002) planes of hexagonal ZnO, which demonstrates that the synthesized ZnO nanowires are of hexagonal wurtzite structure with *c*-axis orientated. To further confirm the crystalline quality of the obtained ZnO nanowires, high-resolution transmission electron microscopy is used. Figure 2(f) shows the HRTEM image of the ZnO nanowires prepared on ITO/PET substrate and it is derived that the lattice spacing is 0.26 nm, corresponding to the distances between (002) planes of hexagonal ZnO, which further supports the aforementioned claim.

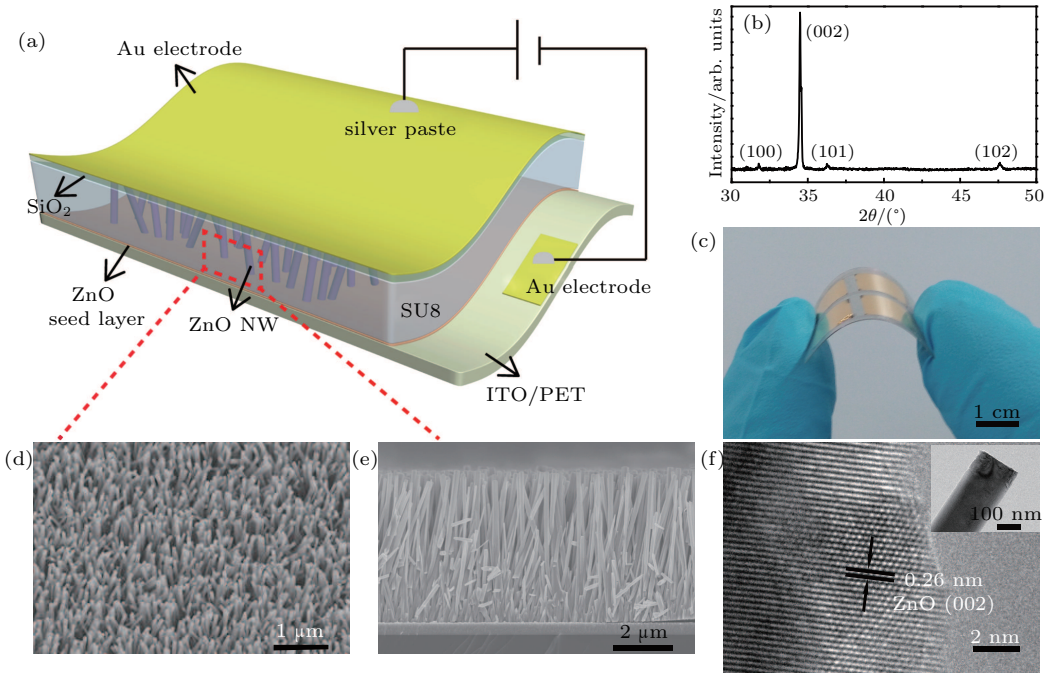



**Fig. 2.** (color online) Schematic diagram (a) and the photograph (c) of the flexible device based on ITO/PET substrate, (b) XRD pattern of the as-synthesized ZnO nanowire arrays, (d) top-view and (e) cross-sectional SEM images of ZnO nanowire arrays grown on PET substrate, (f) HRTEM image of the ZnO nanowire. The inset shows the TEM image of the ZnO nanowire.

### 3.2. Photoluminescence characterization

Figure 3(a) shows the $\mu$-PL spectra of the flexible device based on ZnO nanowires pumped by a 355-nm nanosecond pulsed laser under different laser intensities at room temperature. They clearly show that with increasing pumping intensity, the emission band becomes broader and the emission intensity becomes stronger due to the increase of the density of excitons in ZnO. However, the weak red-shift of the emission band in Fig. 3(a) can be attributed to the electron–hole plasma emission. A single ultraviolet NBE band peaking at $\sim$ 380 nm without visible emission band from the PL spectrum of as-synthesized ZnO nanowires is observed in Fig. 3(b), suggesting that the ZnO nanowire has good crystallinity, and the corresponding setup in the photoluminescence research is shown in the inset of Fig. 3(b).

### 3.3. Electroluminescence characterization

In terms of electrical pumping, forward bias is applied to the flexible MIS device. The current–voltage ($I$–$V$) characteristic curve of the flexible device exhibits typical rectifying behavior as indicated in Fig. 4(c), which indicates that the turn-on voltage is about 2 V. Figures 4(a) and 4(b) show that the EL spectra gradually change with the increase of forward bias voltage applied to such a flexible device. At low applied voltage, the near band emission from ZnO predominantly occurs and a broad emission peak at 395 nm is observed. When the applied bias is increased to 2.7 V, a number of sharp peaks emerge randomly from the shoulder of the broad emission. The full widths at half maximum of these sharp peaks are all about 0.2 nm. When the applied voltage is continuously increased to 2.9 V, the intensity of broad emission becomes stronger, simultaneously more sharp peaks arise randomly in the spectra. The integrated emission intensity against injection current is plotted in Fig. 4(d). It indicates that above a certain threshold current, the integrated emission intensity increases linearly with the injection current increasing, which demonstrates the generation of random lasing. The threshold injection current for lasing is measured to be about 11.5 mA by linear fitting the curve of integrated intensity versus injection current. The threshold injection current ($\sim$ 11.5 mA) is much smaller than that ($\sim$ 50 mA) of the device with a similar structure on rigid substrate.[18] It is notable that almost no substantial visible EL from the flexible MIS device is observed as shown in the inset of Fig. 4(c), which is collected at a driven current of 18.7 mA. The inset in Fig. 4(d) shows the far-field microscope image of the flexible random lasing device captured under an injection current of 20.5 mA. Many distinct light spots in blue-violet randomly distributed can be observed, which prove the UV lasing process in the ZnO nanowires based flexible device.

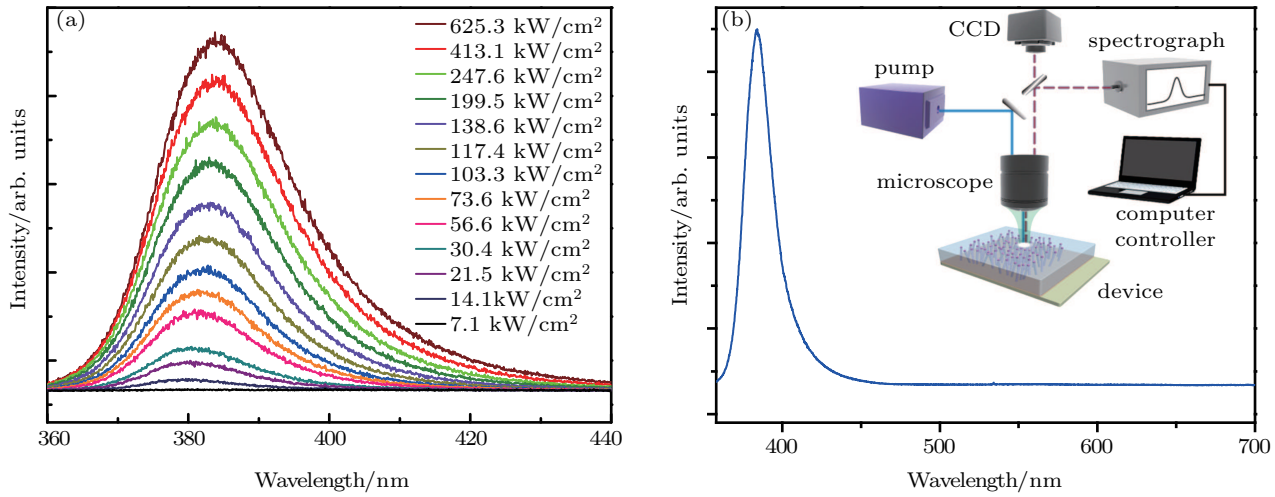



**Fig. 3.** (color online) (a) $\mu$-PL spectra from ZnO NWs-based flexible device grown on the PET substrate excited by a nanosecond pulsed laser in 355 nm, and (b) $\mu$-PL spectrum from 360 nm to 700 nm and the inset showing the setups of photoluminescence experiment.

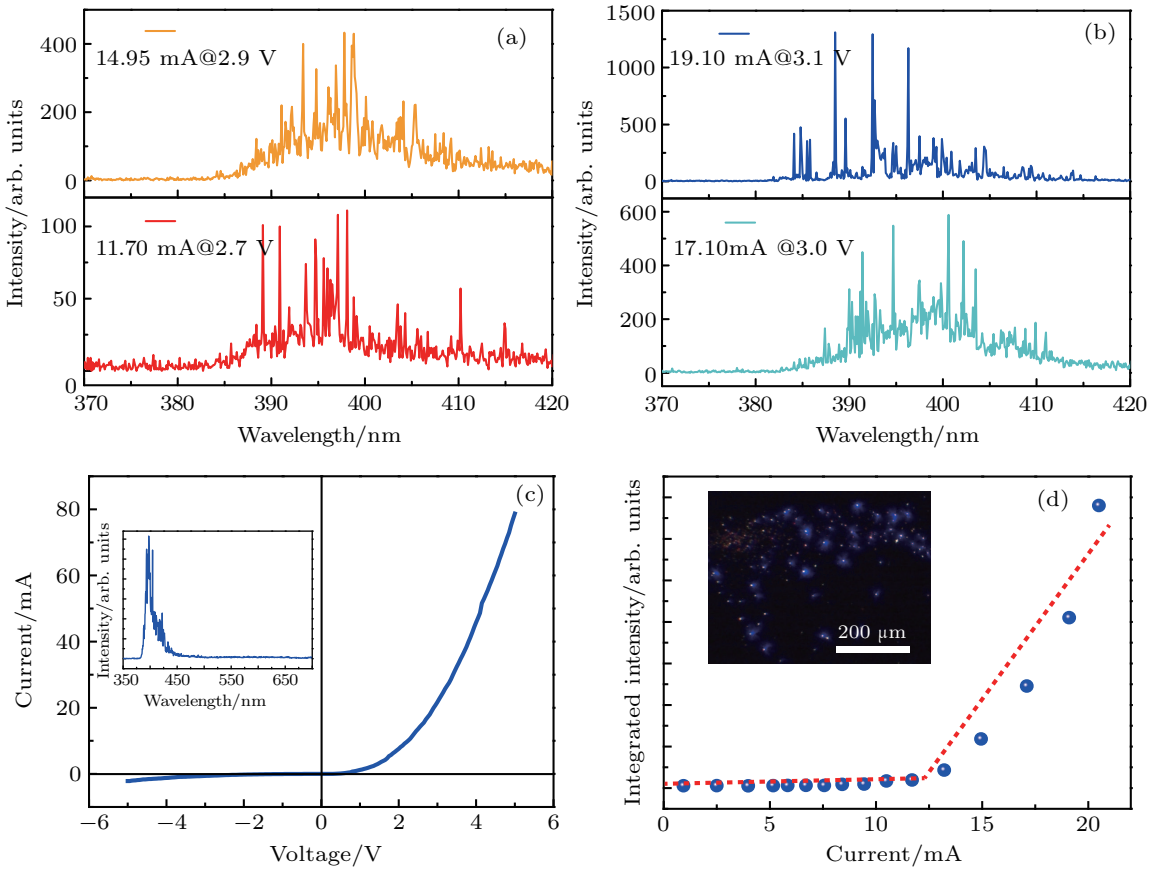



**Fig. 4.** (color online) ((a) and (b)) EL spectra of the flexible MIS device based on ZnO nanowires under different applied voltages/currents, (c) current–voltage curve of the flexible device and inset showing EL spectra from 350 nm to 700 nm of the flexible MIS device under injection current of 18.7 mA, and (d) integrated emission intensity changing with the injection current for the flexible MIS device, and the inset showing the device illuminating under 20.5 mA.

The electroluminescence process could be explained as follows. When a forward bias voltage is applied to the ZnO/$SiO_2$ based flexible MIS device, the electrons transport from ZnO to the ZnO/$SiO_2$ interface and form an electron accumulation region near the interface. In terms of the holes injected into ZnO, the origin of which is still unclear at present, a possible pathway is proposed as follows. For the e-beam prepared $SiO_2$ film, a large number of carrier traps will be introduced into the film in the deposition process. Driven by the applied electric filed, plenty of electrons in ZnO nanowires flow into the $SiO_2$ film and they are trapped in $SiO_2$. Therefore, numerous holes are generated in ZnO nanowires and they mainly accumulate in the region adjacent to the ZnO/$SiO_2$ interface. As a consequence, the EL phenomenon is observed in the region close to the ZnO/$SiO_2$ interface due to electron–hole recombination. Since the accumulation region located in

the ZnO side is extremely thin, scarcely any defect state exists in this region. Therefore, the defect-related visible emission is suppressed to a great extent. On the other hand, it has been reported that the defect states can absorb UV light to some extent, the less defect states will contribute to the enhancement of UV emission.

### 3.4. Random lasing mechanism

In order to better elaborate the mechanism and process of random lasing behavior from such ZnO/$SiO_2$ based flexible device, we delineate a simplified energy band diagram of the MIS structure as illustrated in Fig. 5(a). For simplicity, we assume that some effects can be neglected, such as the free/fixed charges, defect sates in $SiO_2$ film and the interface states between $SiO_2$ and the ZnO nanowires. When applying a forward bias, the conduction and valence band of ZnO bend downward near the ZnO/$SiO_2$ interface. The inclined energy band will accelerate the electrons and holes accumulating at the ZnO/$SiO_2$ interface, and thus form the energy well trapping electrons and holes, respectively. With the increase of applied voltage, the concentrations of electrons and holes increase extremely, which leads to the quasi-Fermi-levels ($E_{Fn}$ and $E_{Fp}$) entering into the conduction and valence bands, respectively. As a result, the energy difference between the $E_{Fn}$ and the $E_{Fp}$ is larger than the bandgap energy ($E_g$), ($E_{Fn} - E_{Fp} > E_g$), which is the condition for generating the stimulated emission in the flexible device.

It is notable that the stimulated emission region limits on the side of ZnO close to the ZnO/$SiO_2$ interface. Since all of the ZnO nanowires are tilted and distributed randomly, each nanowire acts as an independent light emitter. In the propagation process, the light suffers multiple scattering in the plane, and in some cases, the light path will form close-loop resonant cavities as graphically represented in Fig. 5(b), which can effectively enhance the optical gain. When the condition that optical gain is larger than the optical loss inside the resonant cavities is satisfied, random lasing occurs and many discrete sharp peaks emerge in the EL spectra. As shown in Figs. 4(a) and 4(b), the spaces between lasing peaks are not uniform, indicating the different lasing modes generated from randomly formed cavities.

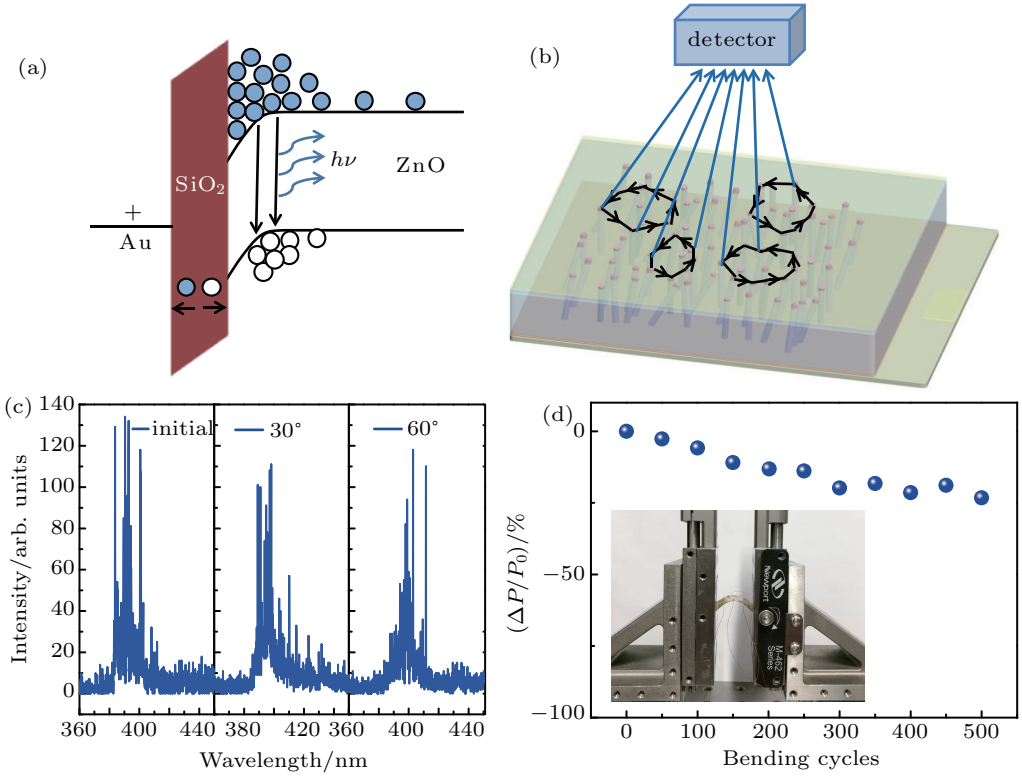



**Fig. 5.** (color online) (a) Energy-band diagram of the ZnO NWs-based MIS device under forward bias, (b) light close-loop cavity randomly formed in the lighting plane, (c) EL spectra of the flexible random laser under different bending degrees, and (d) mechanical robust testing of the flexible random laser, where $\Delta P/P_0$ represents the rate of change in the random lasing intensity, and inset showing the bending setups in the test.

In addition, compared with the previous random laser prepared on rigid substrate,[18] the as-fabricated random laser exhibits great flexibility and excellent luminescent properties. The EL spectra of the flexible random laser under different bending degrees are captured as shown in Fig. 5(c), which indicate that the intensity of the random lasing only shows a slight reduction when the device is bent to 30° and 60°. In order to further investigate the stability of the flexible random laser, we fix the device on a three-dimensional positioning system and bent it back and forth periodically by tuning the rod on

the setup, which is shown in the inset of Fig. 5(d). We define $\Delta P/P_0$ as the rate of change of the random lasing intensity, and the summary of $\Delta P/P_0$ in 500 bending cycles is exhibited in Fig. 5(d). The intensity of the random lasing shows a slight decrease with the increase of the bending cycle, and it almost keeps constant after 300 bending cycles, indicating the remarkable mechanical robustness of the flexible random laser.

## 4. Conclusions

In this work, we prepare a flexible electrically pumped random laser based on ZnO nanowires for the first time. The hydrothermally synthesized ZnO nanowires are of high crystal quality, which is confirmed by TEM, PL and EL characteristics. In order to obtain electrically pumped random lasing, MIS structure devices based on the as-synthesized ZnO nanowires are fabricated. When applying a forward bias, the flexible device exhibits UV spontaneous radiation under a low injection current and random lasing under a sufficiently high injection current. A low threshold current of $\sim 11.5$ mA and high luminous intensity are obtained from the ZnO-based random laser. This work not only demonstrates a flexible electrically pumped random laser based on ZnO nanowires, but also offers an effective way to fabricate various flexible electronic devices.

## References


[1] Li X Y, Chen M X, Yu R M, Zhang T P, Song D S, Liang R R, Zhang Q L, Cheng S B, Dong L, Pan A L, Wang Z L, Zhu J and Pan C F 2015 *Adv. Mater.* **27** 4447

[2] Zhang T P, Liang R R, Dong L, Wang J, Xu J and Pan C F 2015 *Nano Research* **8** 2676

[3] Xu S, Xu C, Liu Y, Hu Y F, Yang R S, Yang Q, Ryou J H, Kim H J, Lochner Z, Choi S, Dupuis R and Wang Z L 2010 *Adv. Mater.* **22** 4749

[4] Yang Q, Wang W H, Xu S and Wang Z L 2011 *Nano Lett.* **11** 4012

[5] Pan C F, Dong L, Zhu G, Niu S M, Yu R M, Yang Q, Liu Y and Wang Z L 2013 *Nat. Photon.* **7** 752

[6] Tian Y, Ma X, Jin L and Yang D 2010 *Appl. Phys. Lett.* **97** 251115

[7] Gao F, Morshed M M, Bashar S B, Zheng Y, Shi Y and Liu J 2015 *Nanoscale* **7** 9505

[8] Zhu H, Shan C X, Yao B, Li B H, Zhang J Y, Zhang Z Z, Zhao D X, Shen D Z, Fan X W, Lu Y M and Tang Z K 2009 *Adv. Mater.* **21** 1613

[9] Dai J, Xu C X and Sun X W 2011 *Adv. Mater.* **23** 4115

[10] Chu S, Wang G P, Zhou W H, Lin Y Q, Chernyak L, Zhao J Z, Kong J Y, Li L, Ren J J and Liu J L 2011 *Nat. Nanotechnol.* **6** 506

[11] Cao H, Zhao Y G, Ho S T, Seelig E W, Wang Q H and Chang R P H 1999 *Phys. Rev. Lett.* **82** 2278

[12] Miao L, Tanemura S, Yang H Y, Lau S P and Xu G 2009 *Phys. Status Solidi* **6** S154

[13] Cao H, Zhao Y G, Ong H C, Ho S T, Dai J Y, Wu J Y and Chang R P H 1998 *Appl. Phys. Lett.* **73** 3656

[14] Vutha A C, Tiwari S K and Thareja R K 2006 *J. Appl. Phys.* **99** 123509

[15] Li H D, Yu S F, Lau S P and Leong E S P 2006 *Appl. Phys. Lett.* **89** 021110

[16] Chu S, Olmedo M, Yang Z, Kong J and Liu J 2008 *Appl. Phys. Lett.* **93** 181106

[17] Li Y, Wang C, Jin L, Ma X and Yang D 2013 *Appl. Phys. Lett.* **102** 161112

[18] Ma X Y, Pan J W, Chen P L, Li D S, Zhang H, Yang Y and Yang D R 2009 *Opt. Express* **17** 14426

[19] Yang H Y, Yu S F, Wong J I, Cen Z H, Liang H K and Chen T P 2011 *ACS Appl. Mater. Interfaces* **3** 1726

[20] Wang C, Nieh C, Lin T and Chen Y 2015 *Adv. Funct. Mater.* **25** 4058

[21] Lu Y, Shan C, Jiang M, Hu G, Zhang N, Wang S, Li B and Shen D 2015 *Cryst. Eng. Comm.* **17** 3917

[22] Tian Y, Ma X Y, Chen P L, Zhang Y Y and Yang D R 2010 *Opt. Express* **18** 10668

[23] Zhang Y, Yang Y and Wang Z L 2012 *Energy Environ. Sci.* **5** 6850

[24] Wang X D, Que M L, Chen M X, Han X, Li X Y, Pan C F and Wang Z L *Adv. Mater.*

[25] Que M L, Zhou R R, Wang X D, Yuan Z Q, Hu G F and Pan C F 2016 *J. Phys.: Condens. Matter* **28** 433001

[26] Boxberg F, Sondergaard N and Xu H Q 2010 *Nano Lett.* **10** 1108

[27] Bao R R, Wang C F, Dong L, Yu R M, Zhao K, Wang Z L and Pan C F 2015 *Adv. Funct. Mater.* **25** 2884

[28] Wang Z L 2012 *Adv. Mater.* **24** 4632